



ELSEVIER

Available online at www.sciencedirect.com

SCIENCE @ DIRECT®

Physica A 327 (2003) 39–43

PHYSICA A

www.elsevier.com/locate/physa

Ultrasound scattering by a vortical flow

A.C. Martí*, S. Varela, A.C. Sicardi-Schifino, C. Negreira

*Instituto de Física, Facultad de Ciencias, Universidad de la República, Iguá 4225,
Montevideo 11400, Uruguay*

Abstract

We report a theoretical and experimental study of the scattering of an ultrasonic wave by a vortical flow. The flow consists of a completely filled cylinder driven by the constant rotation of the two end walls. The angular momentum generated by the disk rotation is concentrated in a strong axial vortex. The scattering of an incident ultrasonic wave allow us to obtain information about the flow. The frequency of the incident wave is assumed to be high in comparison with typical frequencies of the flow. An integro-differential equation is obtained from the full Navier–Stokes equations describing the interaction of the flow and the ultrasonic wave. Using the Born approximation we obtain a wave equation with source which can be numerically integrated or, in some particular cases, be analytically solved. We numerically identify the regions of the vortical flow that contribute most to the scattered wave. The dependence of the scattered pressure on the scattering angle is also studied. Finally, we compare the numerical results with experimental data.

© 2003 Elsevier B.V. All rights reserved.

PACS: 47.32.Cc; 47.35.+i; 67.40.Vs

Keywords: Vortical flows; Sound scattering; Sound-flow interaction

The problem of the flow inside a cylinder with rotating end-walls has received a lot of attention over the years (see for example Ref. [1] and references therein). In the present paper, we analyze this system by means of ultrasound scattering. We restrict our analysis to the case where the angular velocity of the two end walls is the same and the lateral wall is at rest.

Ultrasound scattering by vortical flow has been intensively studied theoretically, experimentally and numerically [2]. In particular, the scattering of sound waves by isolated vortices has been extensively studied [3]. However, studies of vortices of finite

* Corresponding author. Fax: +598-2-5250580.

E-mail address: marti@fisica.edu.uy (A.C. Martí).

length and non-vanishing boundary conditions are scarce. There are previous results [4] that apply to simplified situations where the vorticity is assumed to vanish at the boundaries, typically isolated vortices. In such a case, a linear relation between the scattered acoustic pressure and the vorticity field can be obtained. In this contribution, we consider a more realistic problem where this relation does not hold because the velocity and vorticity do not vanish at the boundaries.

We consider an incompressible flow with velocity $\mathbf{u}(\mathbf{x}, t)$, vorticity $\omega(\mathbf{x}, t)$ and density ρ_0 . We are interested in the interaction of the flow $\mathbf{u}(\mathbf{x}, t)$ with an incident acoustic plane wave with velocity $\mathbf{v}_{inc} = v_0 \cos(\mathbf{k}_0 \cdot \mathbf{x} - v_0 t)$ and the corresponding density ρ_{inc} and pressure p_{inc} . We assume that the amplitude of the perturbation is small compared with the typical velocity scale and the Mach number is also small, $|\mathbf{v}_0| \ll |\mathbf{u}| \ll c = v_0/k_0$. The typical frequency associated with $\mathbf{u}(\mathbf{x}, t)$ is small compared with v_0 . We also assume that the process is isentropic.

In the vortical region, the sound wave induces high-frequency vibrations that produce sound. The full flow can be decomposed as the sum of the flow in the absence of sound and the perturbation produced by the sound wave, $\mathbf{U}(\mathbf{x}, t) = \mathbf{u} + \mathbf{u}'$ and similar decompositions for the density and the pressure.

The interaction of a flow with an acoustic wave can be studied using the Navier–Stokes equations for a compressible medium [4]. Assuming that the incident wave has high frequency and low intensity, it is possible to derive a wave equation with source for the scattered pressure p'

$$\frac{1^2}{c} \frac{\partial^2 p'}{\partial t^2} - \nabla^2 p' = \rho_0 \nabla \cdot ((\mathbf{u} \cdot \nabla) \mathbf{u}) - \nabla \rho' \cdot \frac{\partial \mathbf{u}}{\partial t} + \mathcal{S}(\mathbf{u}, \mathbf{u}'), \quad (1)$$

where

$$\mathcal{S}(\mathbf{u}, \mathbf{u}') = \rho_0 [\nabla^2 (\mathbf{u} \cdot \mathbf{v}_{inc}) - v_{inc} \cdot \nabla^2 \mathbf{u} + \mathbf{u} \cdot \nabla^2 \mathbf{v}_{inc}]. \quad (2)$$

The first term at the r.h.s. of Eq. (1) represents the generation of sound by the velocity field in the absence of any incident wave. The typical frequency of the two first terms is much smaller than that of the incident wave. We focus our attention in the last term representing the interaction of sound and flow.

Since the scattered pressure is small in comparison with the incident pressure, we solve the integro-differential equation using the Born approximation, obtaining

$$p' = p_{inc} + G * \mathcal{S}(\mathbf{u}, \mathbf{v}_{inc}), \quad (3)$$

where $G * \mathcal{S}(\mathbf{u}, \mathbf{v}_{inc})$ is the convolution product of the free Green function, $G(\mathbf{x} - \mathbf{x}', t - t') = [1/(4\pi|\mathbf{x} - \mathbf{x}'|)]\delta(t - t' - |\mathbf{x} - \mathbf{x}'|/c)$, with the source, $s' = \mathcal{S}(\mathbf{u}, \mathbf{v}_{inc})$, where the perturbation has been substituted by the incident wave and the low-frequency contributions have been neglected. The scattered pressure p' at a point \mathbf{x} and time t obtained from Eq. (3) is

$$p' = p_{inc} + \int_V d^3x' \frac{s'}{4\pi|\mathbf{x} - \mathbf{x}'|}, \quad (4)$$

where s' is evaluated at a point \mathbf{x}' and time $t_{ret} = t - |\mathbf{x} - \mathbf{x}'|/c$ and V is the integration volume. Given an arbitrary velocity field, the last equation can be discretized and integrated obtaining the scattered pressure.

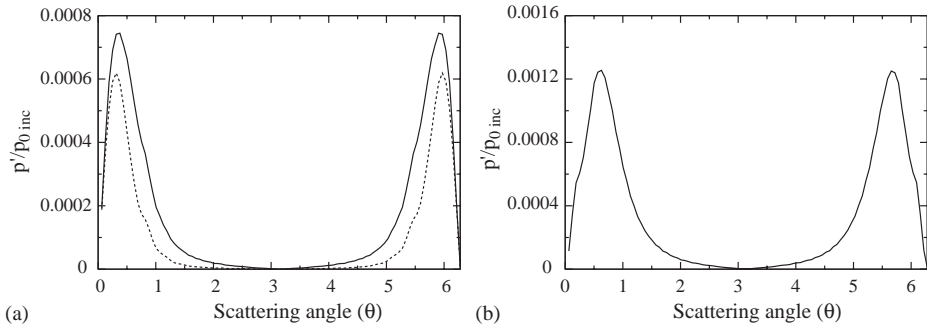


Fig. 1. Maxima of the scattered pressure vs. the scattering angle for different velocity fields. (a) RV (solid line), MRV (dashed line) and (b) NS, $Re = 2550$. The parameter values are: $R_0 = 0.2$, $R/H = 2$, $v_0 = 80$ kHz, $\Omega = 100$ Hz, $N_r = N_\phi = N_z = 100$.

The integration volume is a cylinder of radius R and height H with the top and bottom walls rotating at angular velocity Ω . It is convenient to use cylindrical coordinates r, ϕ, z with the origin at the center of the bottom wall. We have chosen for the discretization a cylindrical grid with elementary spacings, Δ_r , Δ_ϕ , and Δ_z and $N_r \times N_\phi \times N_z$ elements.

Three different velocity fields have been used. The first velocity field correspond to a Rankine vortex (RV) with an abrupt cut-off in the boundary, defined by

$$u_\phi(r) = \begin{cases} \Omega r & r \leq R_0, \\ \Omega R_0^2/r & R_0 < r < R, \\ 0 & r \geq R, \end{cases} \tag{5}$$

where R_0 is the length of the core and $u_r = u_z = 0$. By modifying only the azimuthal velocity in the irrotational region we obtain the modified Rankine vortex (MRV)

$$u_\phi(r) = \frac{\Omega R_0^2}{R^2 - R_0^2} (R^2/r - r), \quad R_0 < r < R. \tag{6}$$

The last one correspond to a numerical three-dimensional solution of the Navier–Stokes equation at moderate Reynolds number [5].

In Fig. 1, we plot the maxima of the scattered pressure vs. the scattering angle for the three velocity fields mentioned. We observe that the curves are similar. As a consequence, this angular dependence is robust against variations of the velocity field. From the analytical expression of the scattered pressure we observe that in the special cases of forward ($\theta = 0$) or back scattering ($\theta = \pi$), due to the symmetry of the source term (see Eqs. (2)–(4)) the scattered pressure must be zero. In addition, it is easy to see that the relation $p_{max}(\theta) = p_{max}(2\pi - \theta)$ holds. However, note that a naive use of the formulae obtained by Lund and Rojas [4] for an isolated vortex does not verify these relations.

It is interesting to calculate the regions of the flow that contribute most to the scattered pressure. After fixating the observation point, the scattered pressure receives

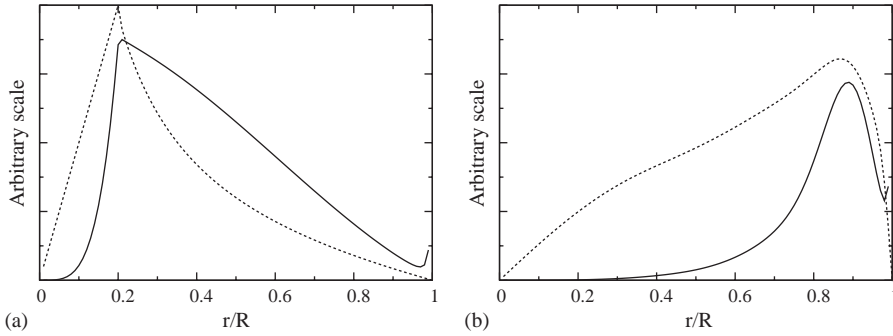


Fig. 2. Spatial dependence of the temporal average of the squared pressure, $p_{cont}^2(r)$, (solid lines) and azimuthal velocity, u_θ (dashed lines). Both magnitudes have been averaged over the scattering angle. (a) MRV and (b) NS. The parameter values are the same as in Fig. 1.

contributions from all the points in the domain at the different times considered. First, we make a temporal average of the squared pressure and next we average in the azimuthal and longitudinal coordinates obtaining $p_{cont}^2(r)$. In Fig. 2, we plot $p_{cont}^2(r)$ for the velocity fields considered. We note that in all the cases, the regions that contribute most are the regions where there are strong variations in the azimuthal velocity and axial vorticity.

The experimental apparatus, a cylindrical vessel filled with water, is similar to the one used by Derroncourt et al. [6]. Two dc-motors are used to drive smooth disks of radius $R = 9.9$ cm at a constant rotation rate. The rotation frequency, $f_{rot} = \Omega/(2\pi)$, varied from 200 to 770 rpm, is controlled by two secondary dc-motors. The Reynolds number, $Re = \rho R^2 \Omega / \mu$, where μ is the viscosity of the fluid, ranges from 2×10^5 to 8×10^5 . The emitter and receiver piezoelectric transducers, made in our laboratory, are located in a plane perpendicular to the rotation axis. We have chosen transducer with a central frequency at 340 kHz in order to obtain a central wave length around 4 cm. This fact minimizes the bubble influences and allow the use of the Born approximation. We work in an impulsional mode to detect the scatter signal of the vortex under better conditions. The experimental results are obtained for three different scattering angles ($\pi/4$, $\pi/2$, and $3\pi/4$). Since the amplitude of the scattered signal of vortex is very small (near level noise), we must amplify it with an ENI (A) power amplifier (20 KHz–10 MHz) and digitalize it using an HP 54600B – 100 MHz oscilloscope. Fig. 3 shows the temporal signal of the scattered sound for different scattering angles. We observe here the main trends obtained in the numerical calculations. Indeed, in Fig. 3(a) ($\theta = \pi$) the signal detected is essentially noise, while for $\theta = \pi/2$ (b) and $\theta = \pi/4$ (c) the amplitude increases according to Fig. 1.

Summarizing, we have obtained the theoretical angular dependence of the scattered pressure and have identified the regions that contribute most to it. The experimental results agree qualitatively with the numerical results. Further work is in progress to make a more quantitative comparison between experiments and theory.

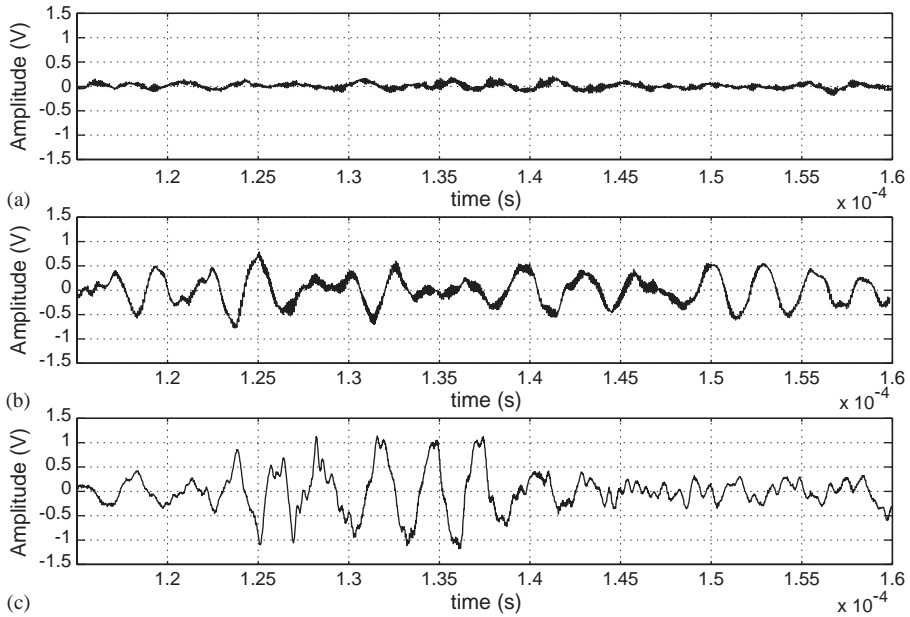


Fig. 3. Time windows of the experimental scattered sound signal, $Re = 7.0 \times 10^5$. (a) $\theta = \pi$, (b) $\theta = \pi/2$ and (c) $\theta = \pi/4$.

We acknowledge support from the CONICYT (FCE-6018) and PEDECIBA (Uruguay). We thank F. Marques (Spain) for providing us with the numerical code to solve the Navier–Stokes equations.

References

- [1] J.M. López, F. Marques, J. Shen, *J. Fluid Mech.* 455 (2002) 263.
- [2] R. Ford, S. Llewellyn Smith, *J. Fluid Mech.* 386 (1999) 305.
- [3] D. Boyer, M. Baffico, F. Lund, *Phys. Fluid 11* (1999) 3819.
- [4] F. Lund, C. Rojas, *Physica D* 37 (1989) 508.
- [5] J.M. Lopez, F. Marques, J. Shen, *J. Comput. Phys.* 180 (2002) 78.
- [6] B. Démoncourt, J.F. Pinton, S. Fauve, *Physica D* 117 (1998) 181.